The Knee 53 (2025) 217–227

Contents lists available at ScienceDirect

The Knee

journal homepage: www.elsevier.com/locate/thekne

AutoCOR: Autonomous condylar offset ratio calculator for post-operative total knee arthroplasty radiographs

Gulsade Rabia Cakmak [a,*], Ibrahim Ethem Hamamci [a], Mehmet Kursat Yilmaz [b], Reda Alhajj [c,d,e], Ibrahim Azboy [b], Mehmet Kemal Ozdemir [c]

[a] International School of Medicine Istanbul Medipol University Istanbul Turkey
[b] Department of Orthopedics and Traumatology Istanbul Medipol University Istanbul Turkey
[c] School of Engineering and Natural Sciences Istanbul Medipol University Istanbul Turkey
[d] Department of Computer Science University of Calgary Calgary Alberta Canada
[e] Department of Health Informatics University of Southern Denmark Odense Denmark

ARTICLE INFO

Article history:
Received 31 March 2024
Revised 24 September 2024
Accepted 2 January 2025

Keywords:
Total Knee Arthroplasty
Machine Learning
Osteoarthritis
Knee
X-ray

ABSTRACT

Background: This study aims to automate the measurement process of posterior condylar offset ratio (PCOR) and anterior condylar offset ratio (ACOR) to improve the Total Knee Arthroplasty (TKA) evaluation. Accurate calculation of PCOR and ACOR, performed manually by orthopedic surgeons, is crucial for assessing postoperative range of motion and implant positioning. Manual measurements, however, are time-consuming, prone to human error, and subject to variability. Automating this process could improve precision in clinical practice.
Methods: We developed AutoCOR, a software system that autonomously calculates PCOR and ACOR by utilizing built-in function, employing k-means clustering, from the OpenCV library for image segmentation. The software detects key anatomical landmarks on true postoperative lateral radiographs. The definitions of PCOR and ACOR are PCO (posterior condylar offset) divided by femoral diameter, and ACOR is defined as ACO (anterior condylar offset) divided by femoral diameter, respectively. We tested the algorithm on 50 postoperative lateral radiographs of 32 patients from the Istanbul Kosuyolu Medipol Hospital, which included data from. The assessment process included calculating the mean, standard deviation and plotting the Bland-Altman plots, comparing AutoCOR's results against ground truth values.
Results: The mean PCOR was 0.984 (SD 0.235) for AutoCOR and 0.972 (SD 0.164) for ground truth values, showing a strong correlation (Pearson r = 0.845, p < 0.0001). The mean ACOR was 0.107 (SD 0.092) for AutoCOR and 0.107 (SD 0.070) for ground truth values, with moderate correlation (Spearman's rs = 0.519, p = 0.0001).
Conclusion: AutoCOR provides accurate measurements and shows potential to reduce variability in TKA evaluation, improving precision in clinical practice.

Abbreviations: TKA, Total Knee Arthroplasty; ACO, Anterior Condylar Offset; PCO, Posterior Condylar Offset; ACOR, Anterior Condylar Offset Ratio; PCOR, Posterior Condylar Offset Ratio; HKA, Hip-knee-ankle; CNN, Convolutional Neural Network; ROI, Region-of-interest; SD, Standard Deviation.

* Corresponding author at: Kavacik Mah. Ekinciler Cad. No: 19, 34810 Beykoz, Istanbul, Turkey.
E-mail address: gulsade.cakmak@std.medipol.edu.tr (G.R. Cakmak).

https://doi.org/10.1016/j.knee.2025.01.002

1. Introduction

Total Knee Arthroplasty (TKA) is a successful surgical operation used for end stage of osteoarthritis. The operation is to improve their functional status on walking and enhance their ability to move [1]. The range of knee flexion is one of the most significant outcome determinants of the Total Knee Arthroplasty (TKA). Maximum flexion smaller than 70 degrees is associated with poor ability to walk, raise from a chair, ascend and descend stairs, whereas maximum flexion greater than 110 degrees is associated with good knee function [2]. Controversy surrounds the relationship between knee flexion range and posterior condylar offset (PCO), with some studies reporting strong correlation while others find no association [2–4]. This controversy provides a research area needed to be further examined in detail, especially considering that PCO is a surgically modifiable factor. Proper assessment of PCO in pre- and postoperative period is important in the clinical practice of orthopedic surgeons [5].

The PCO was initially defined by Bellemans et al. as "maximal thickness of the posterior condyle projecting posteriorly to the tangent of the posterior cortex of the femoral shaft on a true lateral radiograph" [3]. The measurement of PCO requires an accurate knowledge of the specific magnification factor, introducing potential errors from inconsistent radiograph standardization. The errors are likely to originate from uncertain magnification factors and the absence of a reference measurement [6]. To address this, posterior condylar offset ratio (PCOR) and anterior condylar offset ratio (ACOR) were introduced as magnification-independent quantifiable ratios [6,7]. The usage of PCOR, avoiding magnification correction issues, has been emphasized [5]. In a study investigating the relationship between posterior condylar offset ratio (PCOR) and the flexion status of posterior-stabilized (PS) type Total Knee Arthroplasty (TKA), findings indicated that PCOR could serve as a significant parameter for assessing flexion status [6]. Another study revealed a significant association between the anterior femoral offset ratio and the occurrence of anterior knee pain in the postoperative period. Additionally, a correlation was observed between femoral component flexion and reduced anterior femoral offset ratio and increased PCOR. The anterior femoral offset ratio was designated as the anterior condylar offset ratio (ACOR) in this context [7].

PCOR was defined by Johal et al. as "the maximal thickness of the posterior condyle projecting posteriorly to a straight line drawn as the extension of the posterior femoral shaft cortex, divided by the maximal thickness of the posterior condyle projecting posterior to a straight line drawn as the extension of the anterior femoral shaft cortex on a true lateral radiograph of the distal quarter of the femur" [8]. However, in other studies PCOR is defined as PCO divided by femoral diameter [5,7]. ACOR is defined as ACO divided by femoral diameter (Figure 1) [7]. Although PCOR definitions vary, its utility in TKA planning is evident, supported by a mean PCOR value of 0.47 in postoperative radiographs [8].

Figure 1. Illustration of anatomical landmarks and parameters on a lateral knee X-ray. The orange point denotes the anterior edge point of the femoral component, while the red point signifies the posterior edge point. The blue line corresponds to the parallel line to the anterior cortex, and the pink line represents the parallel line to the posterior cortex. The yellow lines (A, B, C) delineate the posterior condylar offset, femoral diameter, and anterior condylar offset, respectively. (For interpretation of the references to color in this figure legend, the reader is referred to the web version of this article.)

Although they are important radiological parameters for successful TKA, the manual measurement/calculation of PCO, ACO, PCOR and ACOR, is not common due to time constraints on busy orthopedic surgeons. To extend the usage of these parameters in clinical settings, we developed a software system, AutoCOR, which can calculate PCOR and ACOR and visualize the landmarks on plain postoperative lateral knee radiographs within seconds using a standard desktop computer. AutoCOR integrates the unsupervised machine learning algorithm (k-means clustering) and image processing techniques (edge detection) to efficiently detect landmarks.

In the current literature, numerous studies regarding the determination of anatomical points on X-ray images using convolutional neural network method exist. One study determines 19 cephalometric landmarks from head X-ray, by integrating image registration and landmark detection through the implementation of ResNet50. The role of the image registration lies on the identification of coarse locations of the landmarks [9]. In a distinct study, orthoroentgenogram segmentation by utilizing the U-Net algorithm to detect ankle, knee and hip joints is conducted to calculate hip-knee-ankle (HKA) angle [10].

In another study, diverse angles are calculated by detecting 9 anatomical points on lower limb X- rays through a two-stage model, which incorporates both first- and second-order detection algorithms. The fundamental concept is to train the second model using region-of-interest patches formed around the points identified by first-order detection models [11].

To sum up the literature review, several studies regarding the landmark detection on lower extremity plain radiographs exist and generally utilized Deep Convolutional Neural Network (CNN). However, to the best of our knowledge no study on autonomous measurement of PCOR and ACOR using image processing, machine learning or deep learning exits in the literature. This situation highlights the necessity of artificial intelligence in this era.

2. Materials and methods

This study has been approved by the Ethics Review Board of Istanbul Medipol University, Istanbul, Turkey (E-10840098-772.02-2381). No signed consent document for each patient was necessary due to anonymization of patient data. This is a retrospective study. The images of 32 patients (26 females, 6 males), who underwent TKA in Istanbul Koşuyolu Medipol Hospital between 2017 and 2021, were utilized. The patients' ages at the time of surgery ranged from 56 to 87. The mean age was 68. The implant sizes differed from patient to patient. The implant size was determined using an appropriate guide while avoiding anterior cortex notching. Intra-operative referencing system utilized was anterior reference system. The TKA type for all patients were PS (posterior-stabilized). Patient selection criteria depended on the availability of a true lateral knee X-ray, captured in the appropriate knee position as per established guidelines.

2.1. The dataset

The choice of imaging modality for the measurement process in the project is grounded in a thorough examination of the literature and current clinical practices [12]. 50 true postoperative lateral knee X-ray images were obtained from the radiology database of Istanbul Koşuyolu Medipol Hospital (Pusula). The images were selected by an arthroplasty surgeon with 16-year of experience. The true radiographs were downloaded in JPEG format. The size of each image is 1378 x 672 px.

2.2. Image preprocessing

The original images are cropped between 500 and 900 pixels in width and 224 to 448 pixels in height. Thus, the size of region-of-interest (ROI) patches are determined as 400 × 224 px (Figure 2b). ROI patches contain only the knee-joint region with femoral condyles. ROI images were processed further with bilateralFilter(), cvtColor() and threshold() methods of

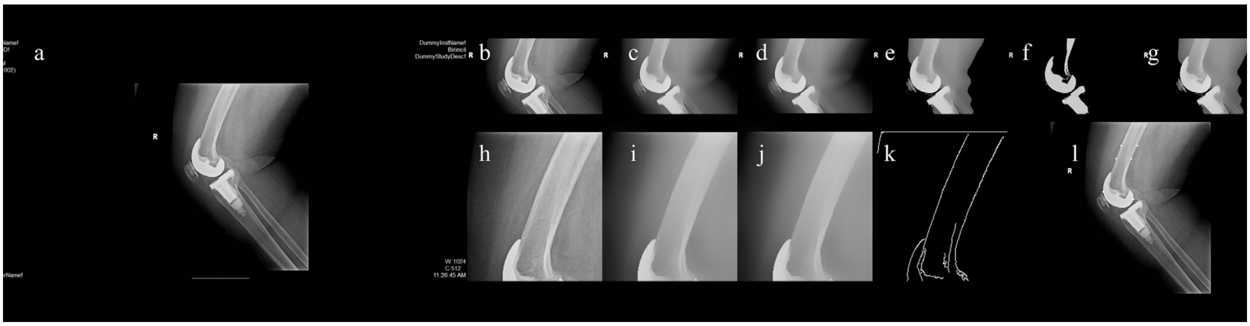

Figure 2. Sequential steps in the image preprocessing algorithm on a sample lateral knee X-ray (a) Sample lateral knee X-ray; **(b)** Slicing the image to a predetermined width and height; **(c)** Applying a bilateral filter for noise reduction; **(d)** Converting the image from RGB to Grayscale; **(e)** Thresholding to enhance image contrast; **(f)** Employing k-means clustering (k = 4) for segmentation; **(g)** Locating contours and creating masks; **(h)** Slicing to isolate the femoral shaft; **(i)** Applying a bilateral filter for noise reduction; **(j)** Converting the image from RGB to Grayscale; **(k)** Implementing Canny edge detection for edge highlighting; **(l)** Extracting 6 anatomical landmarks for subsequent analysis.

OpenCV Library respectively [13]. The aim of the preprocessing step is to make the femoral component prominent on the ROI patch.

a) **bilateralFilter():** Before applying the thresholding method, the image needs to be preprocessed to reduce noise while preserving important structural details. The bilateralFilter() method was selected for this purpose due to its unique blurring mechanism, which combines domain and range filtering. This approach effectively preserves edges while smoothing the image and removing noise. Contrary to traditional blurring methods that may lead to a loss of important edge details, bilateral filtering maintains sharp edges, which is crucial for accurate landmark detection. The d (diameter) is set to 30, sigmaColor and sigmaSpace are set to 100. These parameters are adjusted experimentally to obtain sharp edges and less noise (Figure 2c).
b) **cvtColor():** Image format is converted from RGB to Grayscale (Figure 2d).
c) **threshold():** The combination of THRESH_TOZERO and THRESH_OTSU is used as a thresholding technique (Figure 2e).

2.3. Image segmentation by K-means clustering

The format of each thresholded image is converted to RGB and the image matrix is reshaped to (−1,3). K-means clustering, a built-in function in the OpenCV library, was then employed to segment the image based on color characteristics [13,14]. The main aim is to extract the femoral and tibial components from their surroundings. The criteria-parameter is specified as TERM_CRITERIA_EPS with 10 iterations and an epsilon value of 1. The number of clusters (k value) is determined as 4 and the technique of kmeans() is set to KMEANS_RANDOM_CENTERS. These values are chosen experimentally (Figure 2f).

It is important to note that since K-means clustering is an unsupervised algorithm and implemented as a built-in function in OpenCV, it does not require a separate training and test phase. Therefore, no distinction between training and test data in this context was made. The K-means algorithm groups data points based solely on the inherent structure of the image without prior training [14]. The algorithm is built and tested in Jupyter Notebook [15].

Since the brightness of the components are the highest when compared with other bony and soft tissues. Brightest cluster is the one which has the biggest decimal code indicating its color. In other words, the decimal value closest to (255,255,255) among these 4 clusters belongs to the femoral and tibial component. The model is mainly built on the basis of this rationale.

The contours around the components are detected using the method findContours() with RETR_EXTERNAL option. This option is preferred over other ones (RETR_LIST, RETR_TREE etc.), as it can detect the largest and comprehensive contours, avoiding subsets. The extraction of the femoral component is mediated by a snippet of code based on the comparison of contour areas (Figure 2g).

2.4. Detection of anterior and posterior edge points of femoral component

The extraction of the femoral component allows detecting the edge points of the component on the anterior and posterior side. The coordinates are sorted in ascending and descending order of width (x-axis). The height is sorted in descending order (y-axis). The leftmost and rightmost points are the first element of these sorted lists, respectively. Since the original images were sliced between 500 and 900 px in width and 224 to 448 px in height, the coordinates are re-calculated to make them compatible with original image sizes.

2.5. Detection of anterior and posterior cortex of femoral shaft

The original image undergoes a slicing process to segment the femoral shaft. The image is sliced between left edge point and right edge point with 50-pixel extension to both sides in terms of width. It is sliced down to the level of the edge point in terms of height (Figure 2h). To facilitate landmark detection, the image is processed with Canny Edge Detection, preceded by bilateral filtering and conversion into grayscale format (Figure 2i-k). Thus, an image containing only the anterior and posterior cortex of the femur shaft is created. Subsequently, four strategically selected points are marked at the 100 and 140-pixel levels along the y-axis, with two points positioned on the anterior cortex and two on the posterior cortex. The two parallel lines corresponding to anterior and posterior cortex are formed by utilizing these identified landmarks (Figuer 2l).

2.6. Measurement of femoral diameter, anterior and posterior condylar offset

The results obtained from Steps 2.4 and 2.5 provide the essential anatomical landmarks required for the measurement of Femoral Diameter, ACO (Anterior Condylar Offset), and PCO (Posterior Condylar Offset). The measurement of these parameters is facilitated through the utilization of the "linalg.norm()" function within the Numpy Library [16].

Equation-1 represents the formula to calculate the perpendicular distance between a point and a line. The line equations corresponding to the cortexes of the femoral shaft are computed through the application of the "Line()" method within the Sympy Library. [17].

(Equation-1)

$$\textit{Line passing through two points}:$$

$$P_1 = (x_1, y_1) P_2 = (x_2, y_2)$$

$$\textit{Point}: (x_0, y_0)$$

$$\textit{distance} = \frac{|(x_2 - x_1)(y_1 - y_0) - (x_1 - x_0)(y_2 - y_1)|}{\sqrt{(x_2 - x_1)^2 + (y_2 - y_1)^2}}$$

ACO represents the perpendicular distance between the anterior edge point and the anterior cortex of the femoral shaft, while PCO denotes the perpendicular distance between the posterior edge point and the posterior cortex of the femoral shaft. The femoral diameter is defined as the perpendicular distance between these two cortexes. The measurement of these parameters is conducted in pixel units due to variable zoom levels (0.2 to 0.4) applied to the radiographs. The pixel-based measurements cannot be directly converted into a centimeter-based format.

2.7. Calculation of anterior and posterior condylar offset ratio

As the computation of ACOR and PCOR remains independent of the magnification factor, it ensures robust and accurate results. ACOR is derived by dividing ACO by femoral diameter, while PCOR is obtained by dividing PCO by femoral diameter. Figure 1 illustrates the utilization of these six points and calculation of 2 offset ratios. An important aspect of the proposed model is its versatility, allowing for the analysis of both left and right lateral knee X-rays without the need for prior knee type selection. The model works in the same manner for both left and right knees and autonomously identifies and categorizes the results as per the specified limb type. According to this specification, the results are given appropriately under the respective classes.

2.8. Analysis of the software system AutoCOR

The ground truth ACOR and PCOR values calculated by one orthopedic surgeon were compared with the model outputs. Additional assessment about the accuracy of ground truth values was not performed. The mean, standard deviation, Bland-Altman Plot are the parameters used to evaluate the performance of the AutoCOR.

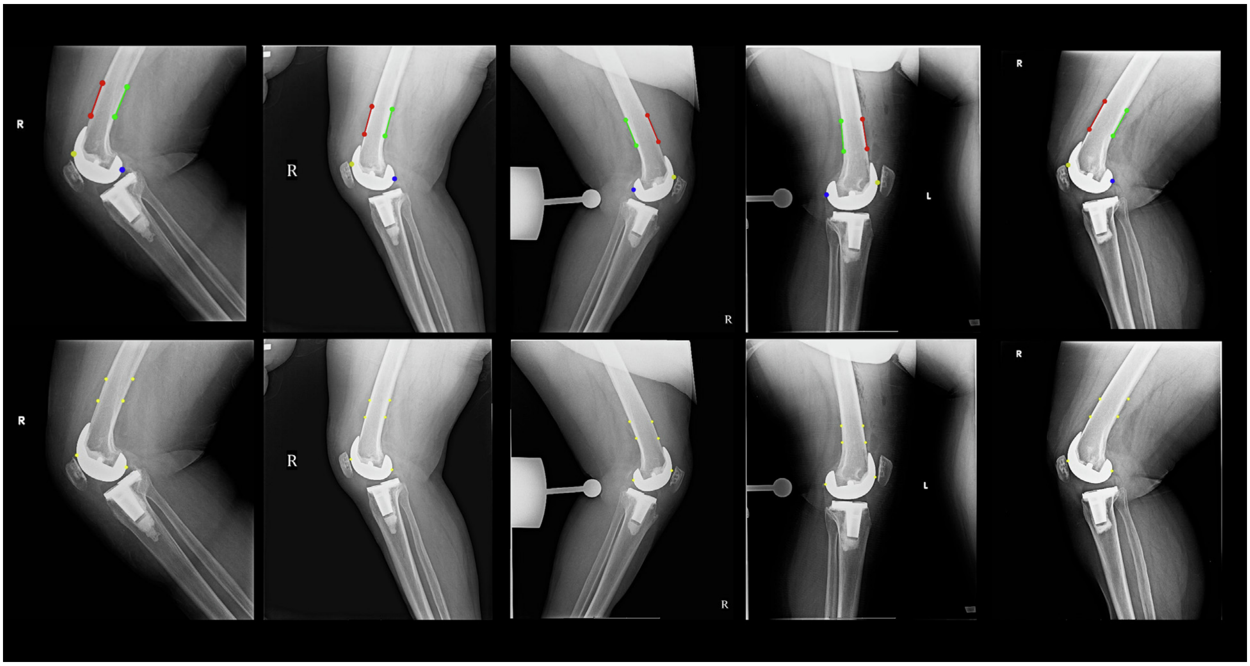

Figure 3. Illustration of a comparison between manually labeled anatomical landmarks (first row), including the anterior and posterior edge points of the component and the anterior and posterior cortex of the femoral shaft, and the corresponding outputs from the model (second row).

2.9. Statistical analysis of model

The statistical analysis was performed on Microsoft® Excel® 2016 MSO (version 16.0.4266.1001) and GraphPad Prism software (version 10.1.2, Boston, Massachusetts, USA). The normality test (The Shapiro-Wilk Test) was applied to assess the distribution of the results before the correlation test. The Pearson and Spearman's correlation coefficient test was applied between the model output and the ground truth values of PCOR and ACOR, respectively.

3. Results

The model outputs, along with manually labeled X-rays used as ground truth values, are depicted in Figure 3. The first row shows the model output images. A total of 6 anatomical points were strategically chosen for the autonomous measure-

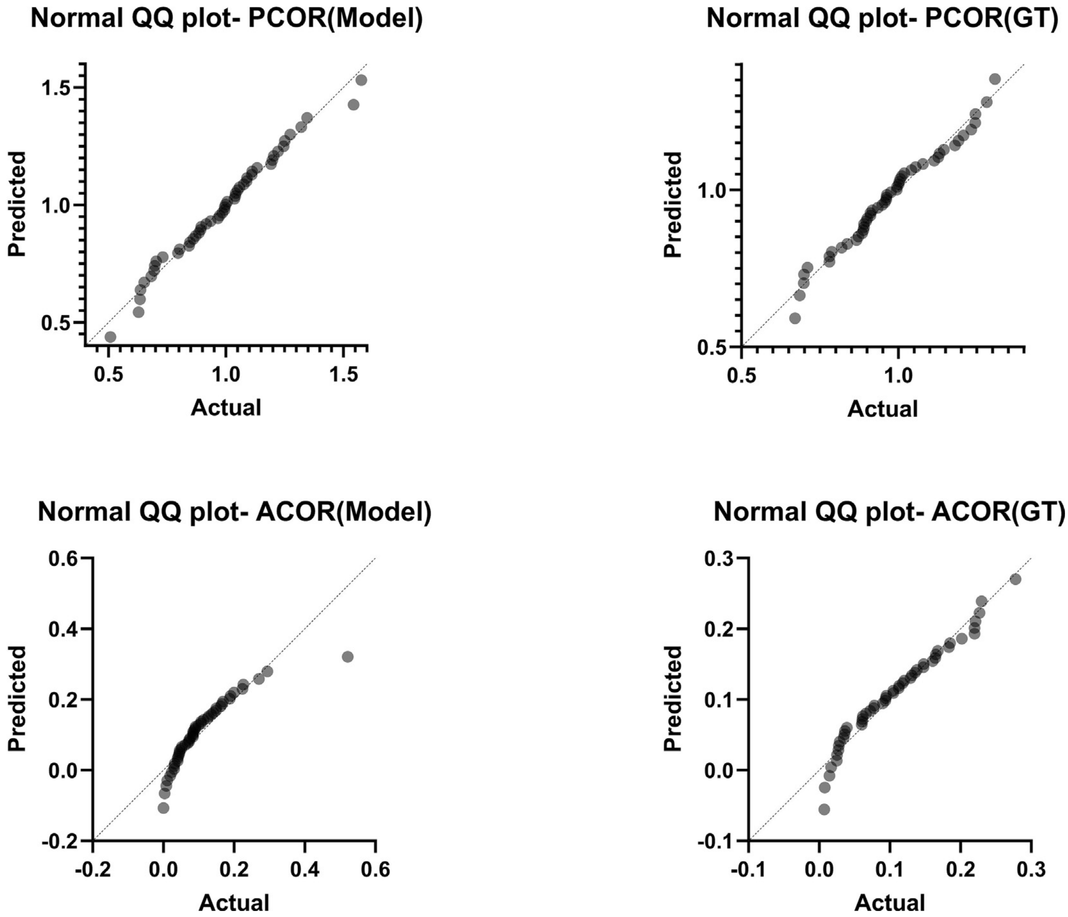

Figure 4. QQ-plots of PCOR and ACOR data, presenting a comparison between the ground truth and model output: These plots aim to compare the distribution of the ground truth values with the model outputs for PCOR and ACOR. The purpose of these plots is to visually assess how well the model's predictions align with the actual measured values. A close alignment along the diagonal line indicates that the model's predictions are in good agreement with the ground truth.

Table 1
Statistical Analysis of PCOR and ACOR Model Outputs and Ground Truth (GT: Ground Truth).

	PCOR (Model)	PCOR (GT)	ACOR (Model)	ACOR (GT)
Number of values	50	50	50	50
Minimum	0.5079	0.6710	0.000	0.007101
Maximum	1.576	1.308	0.5219	0.2777
Range of Values	1.068	0.6366	0.5219	0.2706
Mean	0.9842	0.9721	0.1069	0.1073
Std. Deviation	0.2351	0.1637	0.09191	0.06998
Std. Error of Mean	0.03325	0.02315	0.01300	0.009896
W (Shapiro-Wilk Test)	0.9819	0.9726	0.8252	0.9521
p-value (Two-tailed)	0.6348	0.2941	<0.0001	0.0415
Passed normality test (alpha = 0.05)	Yes	Yes	No	No

ment of PCOR and ACOR. Two points are positioned on the anterior cortex, and two points are positioned on the posterior cortex of the femoral shaft, forming the parallel lines to the cortexes. The remaining 2 points reside on the anterior and posterior edge points of the femoral component.

3.1. Normality tests and statistical analysis

The ground truth and model outputs were tested in terms of normality, by using Shapiro-Wilk Test. Significance level was adjusted to 0.05 (5%). The Q-Q plots were generated for the visualization purpose (Figure 4). The minimum, maximum, mean, and standard deviation for each class were calculated and are reported in Table 1. These statistics were computed for both the raw (ground truth) values and the model outputs for ACOR and PCOR. Table 1 illustrates that the results from the model closely align with the ground truth values, with no significant deviations observed between the two sets of data.

Distribution of the data was evaluated before assessing the correlation between the ground truth and the model results. The mean (SD) results for PCOR model-data and ground truth-data are 0.984 (0.235) and 0.972 (0.164), respectively. The mean (SD) results for ACOR model-data and ground truth-data are 0.107 (0.092) and 0.107 (0.070), respectively.

Table 2
Pearson correlation test results for PCOR data (GT: Ground Truth).

	PCOR (Model) vs.PCOR (GT)
Pearson r	0.8445
95% confidence interval	0.7402 to 0.9092
R squared	0.7133
P (two-tailed)	<0.0001
P value summary	****
Significant? (alpha = 0.05)	Yes
Number of XY Pairs	50

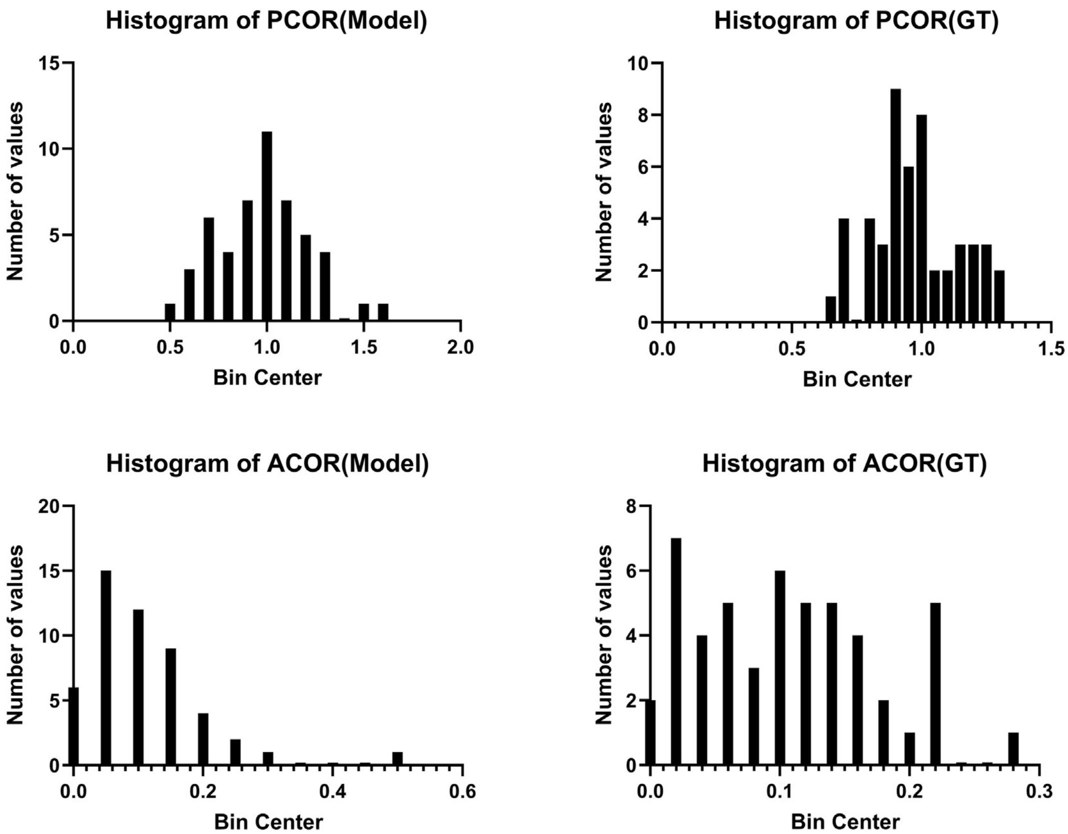

Figure 5. Histograms depicting the distribution of PCOR and ACOR data: These histograms present how the values of PCOR and ACOR are distributed across different ranges for both the ground truth and the model outputs. The purpose of these histograms is to provide a visual summary of the data, allowing readers to quickly assess the overall distribution.

Table 3
Spearman correlation test results for ACOR data (GT: Ground Truth).

	ACOR (Model) vs.ACOR (GT)
Spearman r	0.5188
95% confidence interval	0.2732 to 0.7009
P (two-tailed)	0.0001
P value summary	***
Exact or approximate P value?	Approximate
Significant? (alpha = 0.05)	Yes
Number of XY Pairs	50

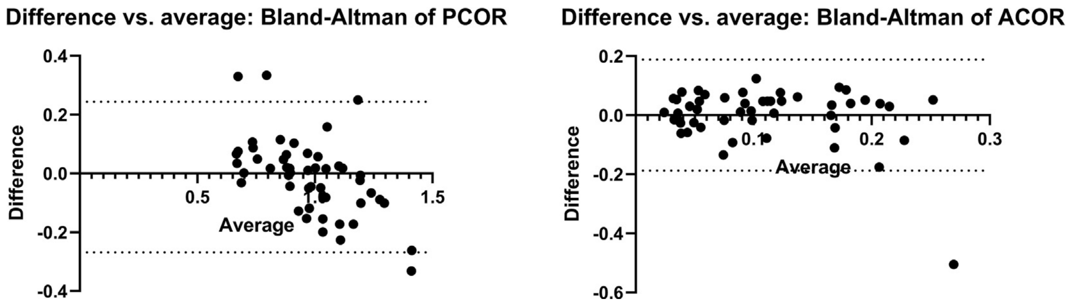

Figure 6. Bland-Altman plots depicting the agreement between PCOR and ACOR data, providing insights into the level of agreement between the ground truth and model output: It plots the ground truth and model output data by calculating the difference between the two against their average. The purpose of these plots is to highlight any systematic bias or differences between the ground truth and the model predictions. It is important to evaluate the reliability of the model in practice.

The Shapiro-Wilk Test resulted in "Normal Distribution" for both model output and ground truth PCOR data (W = 0.98 2p = 0.635 – W = 0.973p = 0.294). The Shapiro-Wilk Test resulted in "Not Normal Distribution" for both model output and ground truth ACOR data (W = 0.825p=<0.0001 – W = 0.952p = 0.042).

3.2. Correlation tests

For PCOR; Pearson Correlation Coefficient Test was applied. The correlation matrix and the p-value were calculated. The correlation between model output and ground truth values is positive and strong (r = 0.845). The Pearson Coefficient appears to be significant at the significance level of 0.05 (p < 0.0001) (Table 2). The histograms of 2 classes are given (Figure 5).

For ACOR; the normality test indicated a non-normal distribution. Due to lack of normality, to assess the correlation Spearman's correlation coefficient test was applied. The correlation matrix and the p-value were calculated. The correlation between model output and ground truth values is positive and moderate (rs = 0.519). The Spearman's Coefficient appears to be significant at the significance level of 0.05 (p = 0.0001412) (Table 3). The histogram of 2 classes are given (Figure 5). The obtained p-value, not equal to zero, signifies the existence of a monotonic correlation and leads to the acceptance of the alternative hypothesis.

3.3. Bland-altman plots

The Bland-Altman analysis was employed to assess the agreement between model outputs and ground truth values for both ACOR and PCOR, as illustrated in the (Figure 6).

4. Discussion

The range of knee flexion is a measure of Total Knee Arthroplasty (TKA) outcome. Although the impact of Posterior Condylar Offset (PCO) on the knee flexion is a controversial point, there are several studies indicating an association. The measurement of PCO in the preoperative and postoperative periods provides an opportunity to the physicians to assess the limb-restoration achieved by TKA. The main concern of this measurement is the lack of standard magnification factor on X-rays (110%–130%). The alterations on the magnification factor result in unstable PCO values in different institutions/ hospitals. In the study conducted by P. Johal et al., a novel parameter, Posterior Condylar Offset Ratio (PCOR), was introduced with an advantage of being independent from the magnification factor [8].

While previous research has established the importance of ACOR and PCOR, there has been no study aimed at developing an automated tool to measure PCOR and ACOR—until now. Our study introduces AutoCOR, a novel model designed to automate the calculation of both PCOR and ACOR on postoperative lateral knee X-rays. This pioneering tool utilizes k-means clustering and advanced image processing techniques to accurately detect the anterior and posterior edge points of the femoral component, as well as the anterior and posterior cortex of the femoral shaft. The model was developed and tested using a dataset of 50 postoperative lateral knee X-rays from Istanbul Medipol Koşuyolu Hospital, with ground truth values manually labeled by an orthopedic surgeon. The results, as shown in Figure 2, demonstrate the model's ability to successfully predict and accurately identify the relevant landmarks, offering a reliable and innovative solution for assessing knee flexion post-TKA.

The PCOR analysis revealed that the mean (standard deviation) of the model output (0.984 (SD 0.235)) closely aligned with the ground truth (0.972 (SD 0.164)), and the Shapiro-Wilk normality test confirmed a normal distribution for both model output and ground truth values (Model: $W = 0.982$, $p = 0.635$; Ground Truth: $W = 0.973$, $p = 0.294$). Similarly, the ACOR analysis showed that the mean (standard deviation) of the model output (0.107 (SD 0.092)) was consistent with the ground truth (0.107 (SD 0.070)). However, the Shapiro-Wilk test indicated a non-normal distribution for ACOR data (Model: $W = 0.825$, $p < 0.0001$; Ground Truth: $W = 0.952$, $p = 0.042$).

Given these results, a Pearson correlation coefficient test was applied to the PCOR data, revealing a strong, positive, and significant correlation between the model output and ground truth values ($r = 0.845$, $p < 0.0001$). For the non-normally distributed ACOR data, Spearman's test showed a moderate and significant correlation ($rs = 0.519$, $p = 0.0001412$). The Bland-Altman plots further confirmed the high level of agreement between the model output and ground truth values, with minimal mean differences observed (Figure 6).

The clinical implications of AutoCOR are profound. By providing an efficient and standardized method for calculating PCOR and ACOR, AutoCOR has the potential to improve the assessment of TKA outcomes across different institutions. This can lead to more consistent evaluations of limb restoration and ultimately enhance patient care. Moreover, the successful correlation between the model's output and ground truth values, as demonstrated by the statistical analyses, suggests that AutoCOR can reliably replicate the accuracy of manual measurements while minimizing human error.

Despite these promising results, several limitations must be acknowledged. The study's limitations include the non-normality of ACOR data and the inability to convert pixel-based measurements (PCO, ACO, and Femoral Diameter) to a centimeter scale due to varying zoom scales in the dataset. To enhance the software's applicability, future work should aim for uniform zoom and magnification factors in X-ray images. In addition to the limitations discussed, it is important to acknowledge several other notable constraints of this study. Firstly, the study was conducted using a relatively small dataset from a single institution. This limitation may affect the generalizability of the results, as data from different centers may exhibit variations that were not captured in this study. Additionally, the ground truth data was provided by a single surgeon, which introduces the potential for bias and limits the robustness of the validation process. Another critical consideration is the potential challenges associated with implementing this software in clinical practice, since it needs to undergo rigorous evaluation and obtain necessary regulatory approvals, such as from the FDA in the United States or the MDR in the European Union.

In conclusion, the key contribution of this study lies in the successful implementation of a fully autonomous method for calculating PCOR/ACOR on postoperative lateral knee X-rays. This pioneering effort introduces a software developed through machine learning and image processing, making it the first of its kind for ACOR and PCOR calculations. This can lead to a shift from manual procedures to an autonomous, efficient, and rapid method, reducing the required effort significantly. Future work will focus on expanding the dataset by collecting radiographs from different institutes, involving multiple orthopedic surgeons to decrease the bias associated with a single surgeon in calculating ground truth values, and further improving the model's accuracy and reliability.

Funding

This research was supported by the TUBITAK (The Scientific and Technological Research Council of Turkey) as 2209-A Project (1919B012003689).

Guarantor

The scientific guarantor of this publication is Gulsade Rabia Cakmak, who is the corresponding author of the article.

Conflict of Interest

The authors of this manuscript declare no relationships with any companies, whose products or services may be related to the subject matter of the article.

Statistics and biometry

No complex statistical methods were necessary for this paper.

Informed consent

Written informed consent was not required for this study because of anonymization of the patient data.

Ethical approval

Institutional Review Board approval was obtained. (Ethics Review Board of Istanbul Medipol University, Istanbul, Turkey (E-10840098–772.02–2381)).

Study subjects or cohort overlap

No study subjects overlap.

Methodology

- retrospective.
- performed at one institution

Data statement

Data can be obtained upon request from the corresponding author, G.R. Cakmak.

CRediT authorship contribution statement

Gulsade Rabia Cakmak: Writing – original draft, Visualization, Software, Project administration, Methodology, Investigation, Funding acquisition, Formal analysis. **Ibrahim Ethem Hamamci:** Writing – original draft, Software, Methodology, Investigation. **Mehmet Kursat Yilmaz:** Writing – review & editing, Supervision, Resources, Data curation. **Reda Alhajj:** Writing – review & editing, Formal analysis. **Ibrahim Azboy:** Writing – review & editing, Supervision, Resources, Project administration, Funding acquisition, Data curation, Conceptualization. **Mehmet Kemal Ozdemir:** Writing – review & editing, Supervision, Conceptualization.

Declaration of competing interest

The authors declare that they have no known competing financial interests or personal relationships that could have appeared to influence the work reported in this paper.

Acknowledgements

We would like to express our very great appreciation to Medipol Koşuyolu Hospital for their support and data provision.

References

[1] Cram P, Lu X, Kates SL, Singh JA, Li Y, Wolf BR. Total knee arthroplasty volume, utilization, and outcomes among Medicare beneficiaries, 1991-2010. JAMA 2012;308(12):1227–36. doi: https://doi.org/10.1001/2012.jama.11153.
[2] Tew M, Forster IW, Wallace WA. Effect of total knee arthroplasty on maximal flexion. Clin Orthop Relat Res 1989;247:168–74.
[3] Bellemans J, Banks S, Victor J, Vandenneucker H, Moemans A. Fluoroscopic analysis of the kinematics of deep flexion in total knee arthroplasty. Influence of posterior condylar offset. The Journal of Bone and Joint Surgery British 2002;84(1):50–3. doi: https://doi.org/10.1302/0301-620x.84b1.12432.
[4] Ishii Y, Noguchi H, Takeda M, Sato J, Toyabe S. Posterior condylar offset does not correlate with knee flexion after TKA. Clin Orthop Relat Res 2013;471(9):2995–3001. doi: https://doi.org/10.1007/s11999-013-2999-2.
[5] Malviya A, Lingard EA, Weir DJ, Deehan DJ. Predicting range of movement after knee replacement: the importance of posterior condylar offset and tibial slope. Knee Surgery, Sports Traumatology, Arthroscopy: Official Journal of the ESSKA 2009;17(5):491–8. doi: https://doi.org/10.1007/s00167-008-0712-x.
[6] Soda Y, Oishi J, Nakasa T, Nishikawa K, Ochi M. New parameter of flexion after posterior stabilized total knee arthroplasty: posterior condylar offset ratio on X-ray photographs. Arch Orthop Trauma Surg 2007;127(3):167–70. doi: https://doi.org/10.1007/s00402-007-0295-x.
[7] Scott C, Clement ND, Yapp LZ, MacDonald DJ, Patton JT, Burnett R. Association between femoral component sagittal positioning and anterior knee pain in total knee arthroplasty: A 10-year case-control follow-up study of a cruciate-retaining single-radius design. The Journal of bone and joint surgery American 2019;101(17):1575–85. doi: https://doi.org/10.2106/JBJS.18.01096.
[8] Johal P, Hassaballa MA, Eldridge JD, Porteous AJ. The Posterior Condylar Offset Ratio. Knee 2012;19(6):843–5. doi: https://doi.org/10.1016/j.knee.2012.03.017.

[9] Song Y, Qiao X, Iwamoto Y, Chen Y-wei. Automatic cephalometric landmark detection on X-ray images using a deep-learning method. Appl Sci 2020;10 (7):2547. doi: https://doi.org/10.3390/app10072547.
[10] Pei Y, Yang W, Wei S, Cai R, Li J, Guo S, et al. Automated measurement of hip-knee-ankle angle on the unilateral lower limb X-rays using deep learning. Phys Eng Sci Med 2021;44(1):53–62. doi: https://doi.org/10.1007/s13246-020-00951-7.
[11] Nguyen TP, Chae DS, Park SJ, Kang KY, Lee WS, Yoon J. Intelligent analysis of coronal alignment in lower limbs based on radiographic image with convolutional neural network. Comput Biol Med 2020;120:. doi: https://doi.org/10.1016/j.compbiomed.2020.103732103732.
[12] Cilengir AH, Dursun S, Sinci KA, Tosun O. Preoperative radiological assessment of the total knee arthroplasty. Forbes J Med 2021;2(2):67–73. doi: https://doi.org/10.5222/forbes.2021.35119.
[13] Bradski G. The OpenCV Library. Dr Dobb's Journal of Software Tools 2000.
[14] Lloyd SP. Least squares quantization in PCM. IEEE Trans Inf Theory 1982;28:129–36.
[15] Kluyver T, Ragan-Kelley B, Pérez F, Granger B, Bussonnier M, Frederic J. et al. and Jupyter development team, (2016) Jupyter Notebooks – a publishing format for reproducible computational workflows. Loizides, Fernando and Scmidt, Birgit (eds.) In Positioning and Power in Academic Publishing: Players, Agents and Agendas. IOS Press. pp. 87-90. doi:10.3233/978-1-61499-649-1-87 doi: 10.3233/978-1-61499-649-1-87>.
[16] Harris CR, Millman KJ, van der Walt SJ, Gommers R, Virtanen P, Cournapeau D, et al. Array programming with NumPy. Nature 2020;585:357–62. doi: https://doi.org/10.1038/s41586-020-2649-2.
[17] Meurer A, Smith CP, Paprocki M, Čertík O, Kirpichev SB, Rocklin M, et al. SymPy: symbolic computing in Python. PeerJ Comput Sci 2017;3:. doi: https://doi.org/10.7717/peerj-cs.103e103.